Geopersia 2023, 13(1): 67-81
DOI: 10.22059/GEOPE.2022.350610.648687

RESEARCH PAPER

Modeling of land subsidence induced by groundwater withdrawal using Artificial Neural Network (A case study in central Iran)

Yasaman Abolghasemi Riseh [1], Ali M. Rajabi [1,*], Ali Edalat [2]

[1] Department of Engineering Geology, Colege of Science, University of Tehran, Tehran, Iran
[2] Graduared from Civil Engineering Department, University of Qom, Qom, Iran

Received: 31 October 2022, Revised: 02 December 2022, Accepted: 12 December 2022

Abstract
Land Subsidence due to the groundwater over-exploitation is a significant problem in some areas which experience urbanization and expansion of agriculture and industry. In this study, the land subsidence of the Aliabad plain of Iran has been modeled using the artificial neural network (ANN) method. In this regard, a multi-layer perceptron has been used to model the land subsidence measured from Sentinel-1 images from 2015 to 2016. Groundwater dropdown, the thickness of alluvial sediments, the aquifer sediments' transmissivity, and elasticity modulus have been considered as four ANN model's inputs variables and land subsidence as a single output. The results show that the ANN model has the ability to predict Aliabad subsidence with good accuracy (R^2= 0.74, R=0.94, RMSE= 0.02 m, MSE = 0.0006). Then a sensitivity analysis was performed in order to determine the impact of input parameters and the results indicate groundwater fluctuations as the most effective one. Model validation was achieved by comparing the ANN results with the calculated land deformation by DInSAR technique. An unused dataset including the four specified input parameters have been used, to assess the generalization of the ANN model. The model produces a proper prediction of land deformation with the new dataset.

Keywords: Artificial Neural Network, Land Subsidence, Groundwater Over-Exploitation, Groundwater Level Dropdown.

Introduction

Land subsidence is a gentle downward movement and/or sudden falling of distinct segments of the ground surface. This phenomenon occurs following the principal causes including aquifer system compaction, drainage of organic soils, underground mining, hydro-compaction, natural compaction, sinkholes, and thawing permafrost (Galloway et al., 1999). Ground subsidence may occur by natural processes such as the dissolution of limestone or earthquake. Earthquake is one of the significant triggers of land subsidence in Japan which from 2009 to 2019 experienced 70 times major earthquake (Na et al., 2021). Also, ground subsidence takes place by human activities like coal mining. The coal industry has played an important role in the development of the Korean economy since the 1960s and ground subsidence around abandoned areas of coal mines imposes fatalities and property loss (Oh et al., 2011). However, subsidence due to the extraction of fluids such as water, crude oil, and natural gas from subsurface formations perhaps is the best recognized of all causes of land subsidence induced by human activities and natural processes. Land subsidence due to over extraction of groundwater plays a direct role in land subsidence by causing the compaction of susceptible aquifer systems (Galloway & Burbey, 2011). Over 150 major cities in the world

* Corresponding author e-mail: amrajabi@ut.ac.ir

have experienced tremendous land subsidence (Hu et al., 2004) and many areas of subsidence caused by the pumping of groundwater have been widely identified in the world such as Mexico City (Calderhead et al., 2012), Shanghai (Hu et al., 2004), Tianjin (Lixin et al., 2011), Antelope Valley, California (Galloway & Burbey, 2011), Bankok (Phien-Wej et al., 2006), Rafsanjan (Mousavi et al., 2001), Mashhad (Motagh et al., 2007), Arak (Rajabi & Ghorbani 2016; Jahangir et al., 2020), Tehran (Mahmoudpour et al., 2015) and Qom (Edalat et al., 2020). Land subsidence is a matter of great concern from different aspects involving socio-economic and environmental damage and safety problems in affected areas (Gambolati & Teatini, 2015). Land subsidence can, directly and indirectly, impairs infrastructure and buildings, accelerates inundation, decreases aquifer storage capacities, builds sinkholes, degrades both agricultural and urban land (Hu et al., 2009; Pirouzi et al., 2014), disturbs lifelines (road, railway, pipelines) and weakens sustainable water management (Galloway & Burbey, 2011). As land subsidence has a gentle process it goes unnoticed especially at the beginning stages and only be discovered after severe damage has taken place (Gambolati & Teatini, 2015). Therefore, studying and precise estimation of this complex geological phenomenon supplies beneficial information for controlling and diminishing the impacts of such drastic hazards. Several studies have been conducted around land subsidence with different approaches. Satellites based on remote sensing techniques improved the monitoring methods and have been used in monitoring land subsidence. In the last years, several studies have been performed subject to monitoring methods such as Environmental Satellite Advanced Synthetic Aperture Radar (ENVISAT ASAR) of land subsidence due to groundwater withdrawal (Dehghani & Nikoo, 2019). Differential interferometry Synthetic Aperture Radar (DInSAR) is one such technique that has shown its ability to produce accurate measurements of land subsidence (Edalat et al., 2019). However, although the remotely sensed techniques have their advantages over traditional in situ observation in land subsidence measurement, there is a lack of accurate information on noisy pixels (Dehghani et al., 2013). According to Calderhead et al., (2011), numerical models are quite functional tools to estimate the land subsidence caused by groundwater level decline. Mahmoudpour et al., (2015), simulated the groundwater level and land subsidence in southwest Tehran by end of 2004 by PMWIN (Modflow for Windows) in good agreement with the measured values. Also, their prediction model of land subsidence through the end of 2018 illustrated that subsidence will reach to 33 cm by 2018. Zhao et al., (2021) have conducted research to predict land subsidence due to groundwater level decline in Ningbo urban area, China. A coupling model of groundwater and land subsidence was developed to predict the land subsidence caused by water withdrawal. Numerical results show that the pore confined water in Ningbo urban area has good conditions and strong water level recovery ability.

Many studies of land subsidence have been done by numerical and hydraulic approaches, these numerical models need significant historical and or real-time data regarding aspects of groundwater or subsurface water, which makes these methods more difficult to use in data sparse regions (Arabameri et al., 2020). Soft computing models are beneficial tools to predict land subsidence. Machine learning algorithm (MLA) can create better multi-dimensional models than conventional and numerical methods related to non-linear data with complex interactions and involving missing values (Knudby et al., 2010). For instance, Artificial Neural Networks (ANNs) have been used in some studies to assess land subsidence (Taravatrooy et al., 2018). Dehghani et al., (2013), using a multilayer perceptron neural network to evaluate land subsidence rate with considering six hydrological variables. In order to obtain accuracy of land subsidence rate, they clustered forcing data and trained different models for each cluster and combined their results of estimations. Dehghani et al., (2019), accomplished a research to monitor land subsidence in three case studies (Varamin Plain, Neyshabour Plain, and Shahriar Plain). While low correlation between groundwater decline in some piezometers with land

subsidence they use data mining methods (neural network and support vector machine) to investigate the relation between land subsidence and other geology and hydrogeological factors. Rahmani & Ahmadi, (2018) used 11 TerraSAR-X images to calculate land subsidence due to groundwater withdrawal and its rate in the southwest plain of Tehran. They predicted the amount of subsidence for the twelfth month by analyzing time series with the help of a neural network. Arabameri et al., (2020) introduced a new ensemble method called ANN-bagging to predict land subsidence of Semnan plain. It uses bagging as an ensemble-classifier of an artificial neural network. The produced land subsidence susceptibility mapping indicated that 5.7-12.6% of the Semnan plain suffers from very high land subsidence susceptibility that is in an agricultural area with high groundwater decline.

Despite the significance of land subsidence in Qom province, a limited number of researches have been accomplished on this issue. Rajabi, (2018), evaluated land subsidence over a period of 12 years in some parts of Aliabad plain due to the large exploitation of groundwater by using Plaxis3D. The results indicated that the area experienced 0-76 cm land subsidence corresponding to a 26.35 m decline in groundwater level. Edalat et al., (2019), by using the DInSAR method investigated the land subsidence of the Aliabad plain caused by groundwater level decline. The satellite images between 2015 and 2016 and groundwater level from 2002 to 2015 were used to study land subsidence. The results indicated that the Aliabad plain experienced a continuous vertical displacement of about 178 mm/year from 2015 to 2016.

This study is subject to modeling the land subsidence from 2015 to 2016, due to groundwater dropdown with a different approach from previous studies in Aliabad Plain. According to the successful performance of the ANN method in geoscience, an artificial neural network model has been considered for land subsidence prediction. In this regard, a multi-layered perceptron neural network has been applied. Hydrogeological and groundwater table information from 2009 to 2016 has been used to model the land subsidence of the Aliabad plain.

Overview of the study area

Aliabad plain of Qom is located in the Markazi and Qom provinces in the range of 34˚ 42′ 27″ to 35˚ 9′ 27″ north latitude and 50˚ 8′ 3′ to 51˚ 3′ 24″ east longitude. Aliabad plain is parts of the central Iran zone and the Urmia-Dokhtar volcanic belt. The sedimentary basins of this region, simultaneously with the formation of elevations during the final phase of Alpine orogeny, along with many older sedimentary basins, lost their connection with the sea and became vast lands in which evaporative sediments such as gypsum and salt with clay and marl has been deposited (Darvishzadeh, 1991). Volcanic rocks and oligomiocene limestones and pliocene conglomerates have formed moorlands and mountains in the northern half of the region in a north-west-south-east direction. The southern half of the Aliabad plain has formed from a series of syncline and anticlines with gentle to steep slopes. In addition, there is no trace of a major fault close to the study area but the inferred Alborz fault (Zamani-Pedram et al., 2002). The studied plain is located among terraces and mostly in clay flats, mainly silt and clay. The alluvial sediments of Aliabad plain result from the operation of rivers in it, which have become finer grain alluvial sediments by reducing the discharge of these rivers from east to west. The subsurface sediments of the region mostly consist of silt and clay, and in the highlands, conglomerates with interlayers of micro conglomerates. The river course of the Qomrud and Qareh-chay rivers, situated in the southern part of Aliabad plain, separates the roughness and mountains of the northern half of the southwestern mountain range of the Qom region (Yazdan Mountain with a height of 1630 meters above sea level). The plain with an area of 1794 km^2 and its arid climate (the annual mean temperature around 18 ˚C and mean annual precipitation less than 200 mm) is faced to land subsidence due to the over-exploitation of groundwater. Its unconfined aquifer with an area of about 1630 km^2 is a part of the Saveh basin. Aliabad plain's aquifer is one of the few freshwater

sources northwest of Qom province, which is recharged with the permanent Qareh-chay River. In the aftermath of the construction of the Al-Ghadir dam in 1994 near the Aliabad village the river that had been one of the most vital sources of aquifer recharge and irrigation of agricultural lands in this region went dry for most of the years and turned into a seasonal river (Water Resources Report of Saveh Study Area, 2013). Therefore, deep and semi-deep wells are used as the water supply for agricultural and drinking purposes instead of rivers and Kanat which were approachable in the past. This leads to a depression in the aquifer water level. Figure (1) demonstrates the area of Aliabad plain and the study area and Figure (2) indicates alluvial sediments along AA′ profile from west of the plain to east.

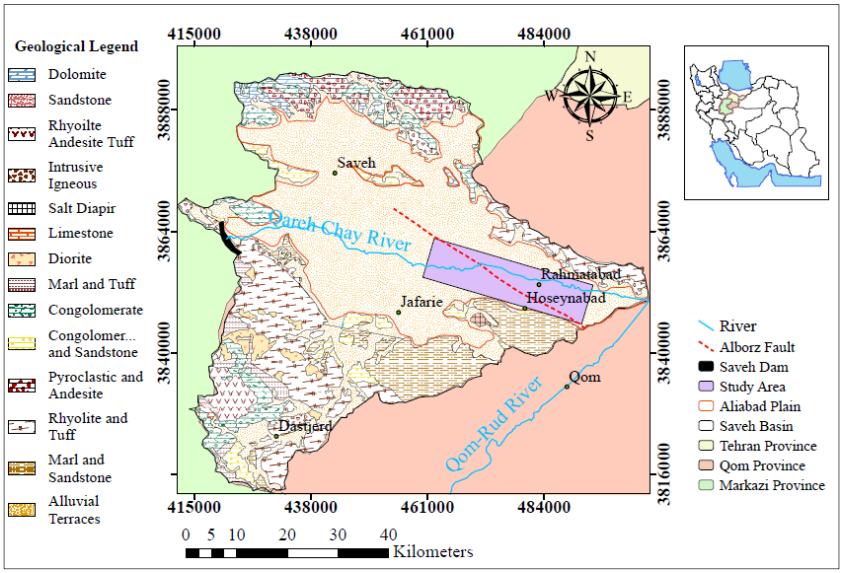

Figure 1. Aliabad plain and the study area

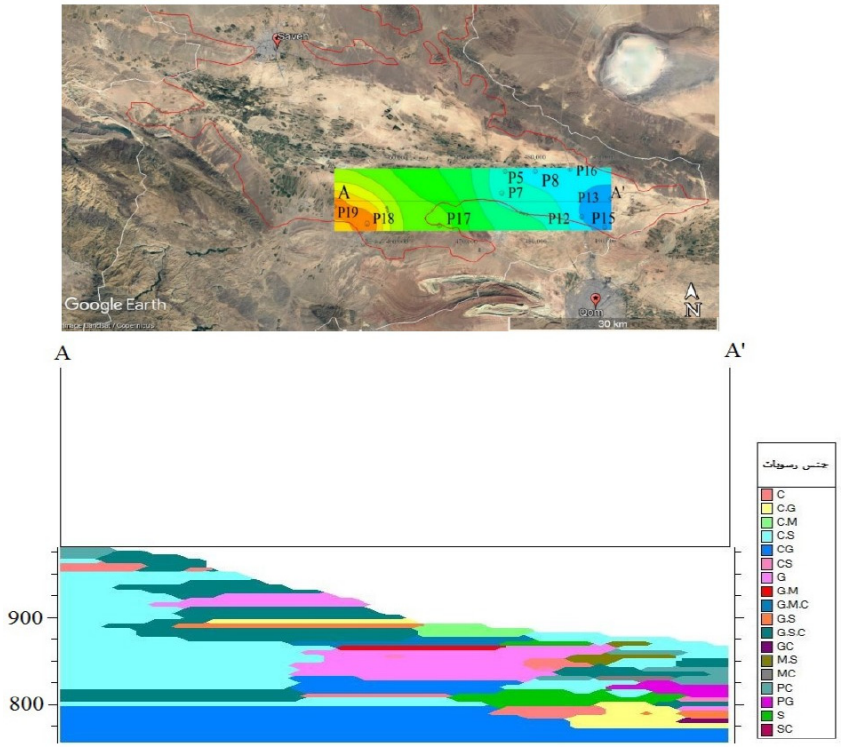

Figure 2. Alluvial sediments along AA′ profile

Data and Methods

The objective of this study is to develop a model for land subsidence analysis. The implemented methodology could be distinguished into three steps: (a) the first step involved defining the dependent and independent (geological, hydro-geological, and geotechnical properties of the study area) variables and the investigation of the spatial and temporal inclination of groundwater changes (b) normalization and data processing, and the final step (c) construction of the ANN models, and model validation. Figure (3), demonstrates the flowchart of the applied methodology and then these steps are described in more detail in the following. In the following the first 2 steps are described in dataset section and then step 3 is discussed in artificial neural network section.

Dataset

Aliabad Plain faced to lack of good geo-environmental information of the plain. As a result, in order to create a land subsidence model by ANN method, the existing data in some part of the plain have been used. In this regard, a geometric study area with the best distribution of piezometers, the coverage of the interferogram images, and sufficient hydrological and geological information has been considered. Figure (4) illustrates the study area, the distribution of piezometers, and groundwater level contour lines. The input factors have been shown in figure (5). Aliabad aquifer developed in alluvial deposits that consist of unconsolidated rock, chiefly clay and silt. According to Todd and Mays, (2005), the Aliabad aquifer is placed in water course categories, and alluvial sediments are essentially from existing rivers. The thickness of alluvial sediments drops from west to east of the plain (figure 5-c). Groundwater changes have been obtained from observation wells from 2009 to 2015 with a maximum decline of 15 m in the study area (figure 5-b). The transmissivity of sediments is varied from less than 200 to approximately 3000 m^2/d near the Qareh-chay riverbank and the *E* modulus is changed from 30 to 50 N/mm^2 in the study region (figure5-a, d).

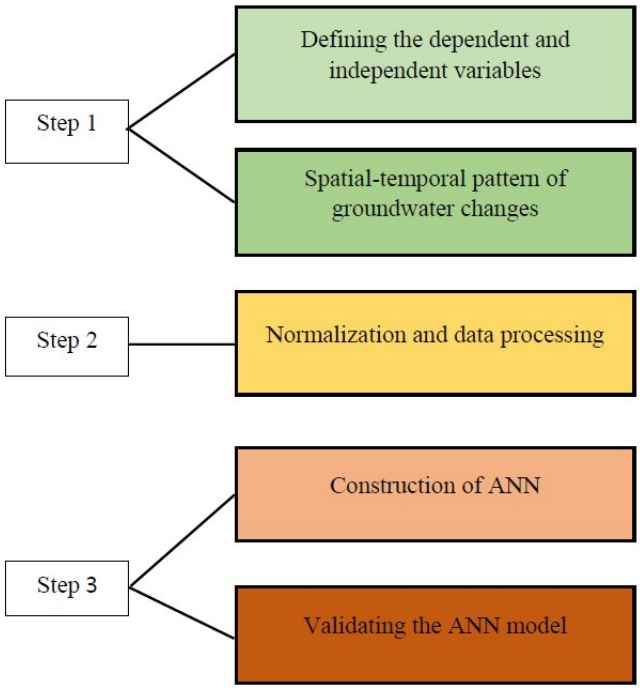

Figure 3. Flowchart of the applied methodology

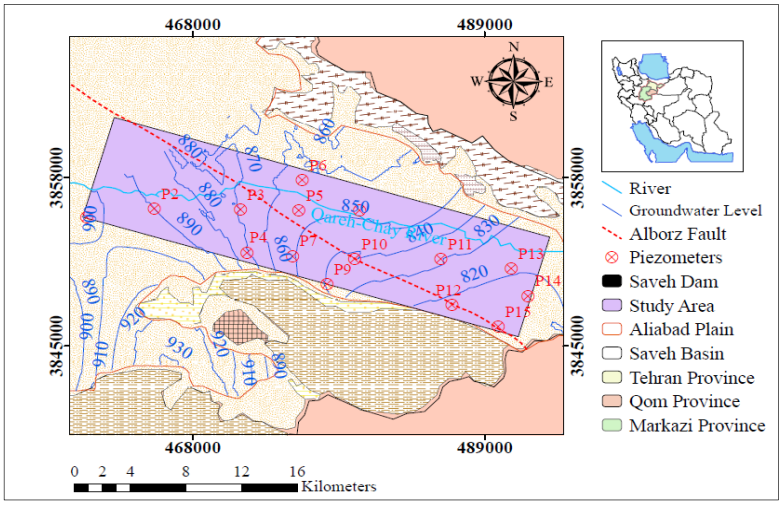

Figure 4. Study area, groundwater level contours line, and the distribution of piezometers

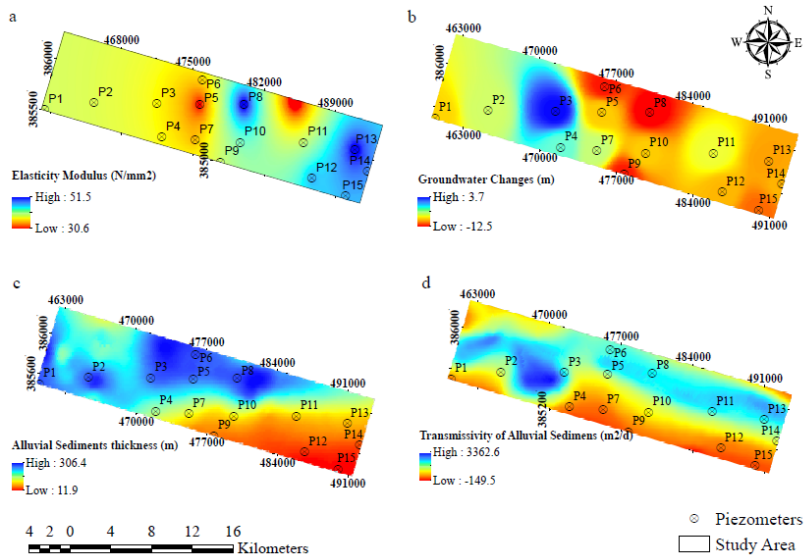

Figure 5. Distribution of independent inputs variables in the study area, a) E modulus, b) Groundwater changes, c) Alluvial sediments thickness, d) transmissivity of sediments

Artificial Neural Network

Artificial Neural Networks (AAN) are known as machine learning models that are inspired by the complex neurons' information processing of the human's brain (Kia, 2016) and have become relatively competitive with conventional regression and statistical models regarding usefulness (Dave & Dutta, 2014).

Architecture of ANN

In this study, a feed-forward back-propagation multi-layer perceptron with 2 hidden layers and 18 neurons in each layer with the Levenberg-Marquard algorithm has been applied. In addition, the logsig, tansig, and purelin as the transition functions for each layer have been considered, respectively. The developed MLP model took into account 4 input factors including groundwater changes, sediments thickness, transmissivity coefficient, and elasticity modulus on subsidence. Figure (6), indicates the schematic architecture of created ANN model.

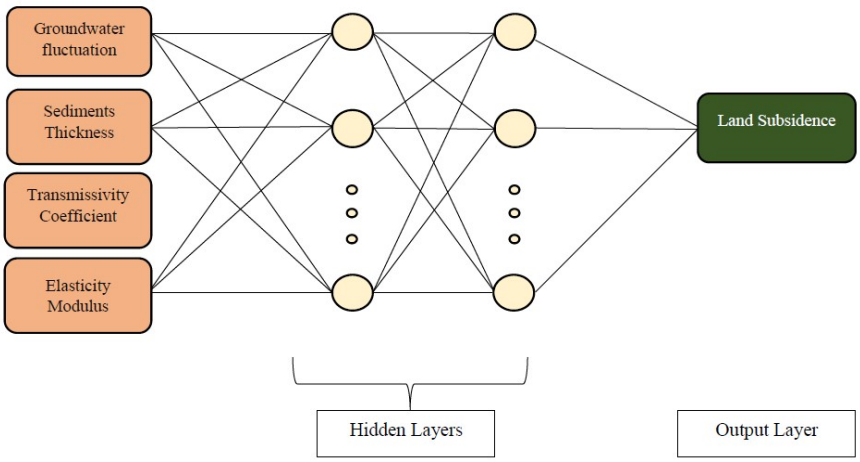

Figure 6. Architecture of ANN model

Division of Dataset

There are 6440 points which have information of the thickness of alluvial sediments, the transmissivity coefficient, elasticity modulus, groundwater changes, and land deformation. A 6440×4 matrix for inputs parameters and a 6440×1 matrix for output factor has been created. The dataset has divided randomly into three sets including 70% (4508 points) of data for training, 15% (966 points) for validation data, and 15% (966 points) for test data. The indicators of ANN inputs possess disparate dimension, and their discrepancy of magnitude are comparatively large. Neural network training works faster more efficiently by performing certain data preprocessing (Jayalakshmi & Santhakumaran, 2011). In order to make each factor in an equal scale, all the parameters (inputs and output) of the neural network are normalized quantitatively, as given in formula (Gunn, 1998), so the values put in the range of 0 and 1 (relation 1).

$$x_{normalized} = \frac{x_i - x_{min}}{x_{max} - x_{min}} \qquad (x_i \varepsilon X | X \varepsilon A) \qquad (1)$$

Performance Evaluation

In this study, for evaluating the model performance and comparing the results, four statistical criteria have been applied. These criteria include Root Mean Square Error (RMSE), Mean Square Error (MAE), coefficient of determination (R^2), and coefficient of correlation (R) that have been used to evaluate the models (relationships 2 to 5).

$$RMSE = \sqrt{\frac{1}{n}(Z_i - \hat{Z}_i)^2} \qquad (2)$$

$$MSE = \frac{\sum_i^n (\hat{Z}_i - Z_i)^2}{n} \qquad (3)$$

$$R^2 = \frac{\left[\sum_{i=1}^n (P_i - P_{ave})(Q_i - Q_{ave})\right]^2}{\sum_{i=1}^n (P_i - P_{ave})^2 (Q_i - Q_{ave})^2} \qquad (4)$$

$$R = \frac{\sum_{i=1}^n (X_{a,i} - \overline{X_a})(Y_{b,i} - \overline{Y_b})}{\sqrt{\left\{\sum_{i=1}^n (X_{a,i} - \overline{X}_a)^2 \sum_{j=1}^n (Y_{b,j} - \overline{Y}_b)^2\right\}^{1/2}}} \qquad (5)$$

Results and Discussion

In the current research, the artificial neural network model has been trained by 4508 of all real datasets and remained data is devoted to testing and validation data. The artificial neural

network for modeling land subsidence has been developed using MATLAB R2018b. According to obtained results, the plain has experienced maximum land subsidence of about 15 cm close to the P_1 and P_2 piezometers area with agricultural and municipal land use. Due to long-term groundwater level decline and compaction of silt and clay layers (aquitards), the region encounters relatively large land subsidence. Table (1) indicates the results of the optimal ANN model of land subsidence in the Aliabad plain of Qom.

Table (1) exhibits the evaluation parameters including determination coefficient, correlation coefficient, mean square error, and root mean square error for training, validation test, and total data sets in order to analyze the artificial neural network model. According to the obtained value of RMSE for the total data, the artificial neural network model has calculated the ground subsidence at each point with an average error of 2 cm. In addition, R^2= 0.74 for training dataset shows that the model has trained expertly but the results of the test and validation indicates that the model has learned the complex relationships between inputs parameters. Figure (7) presents the performance of training, testing and validation processes during model learning. The declining trend of the graph of all three sets and their affinity with each other shows the proper performance and generalizability of the ANN model. In addition, according to the presented figure, the model has reached the optimal model with the least error in epoch 370.

Figure (8) shows the relationship between the values obtained from the artificial neural network model and the measured subsidence values. The value of R= 0.94 and R^2= 0.74 indicates a good approximation of the model and the predicted values are very close to the real values.

Figure (9) shows the histogram of error frequency. According to the presented illustrated, the histogram has a normal distribution and the overestimation and underestimation values are almost the same at different points, and the absolute average error is equal to μ=0.0175. In the following figure (10), the results of ANN subsidence model in the training, test, validation phases, and total data are given in comparison with real data.

Table 1. MLP neural network results

Results	Train Data	Test Data	Validation Data	All Data
R^2	0.74	0.8	0.78	0.74
R	0.95	0.94	0.93	0.94
RMSE(m)	0.02	0.02	0.02	0.02
MSE	0.0006	0.0004	0.0004	0.0006

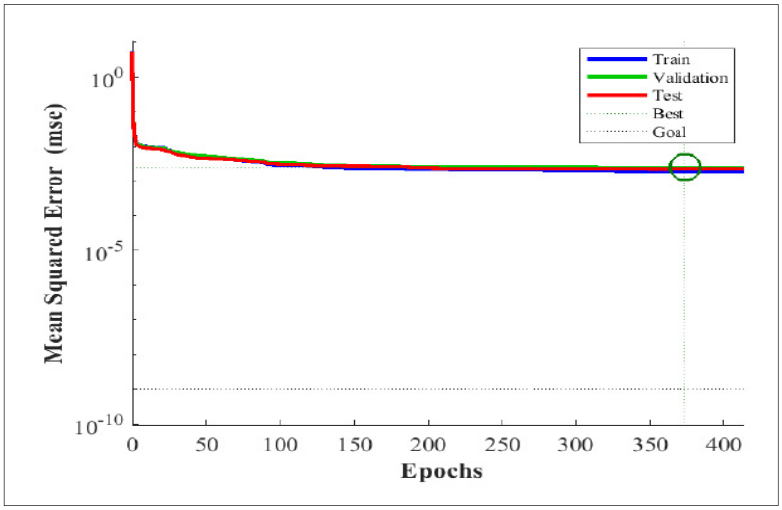

Figure 7. Performance of training, testing and validation processes

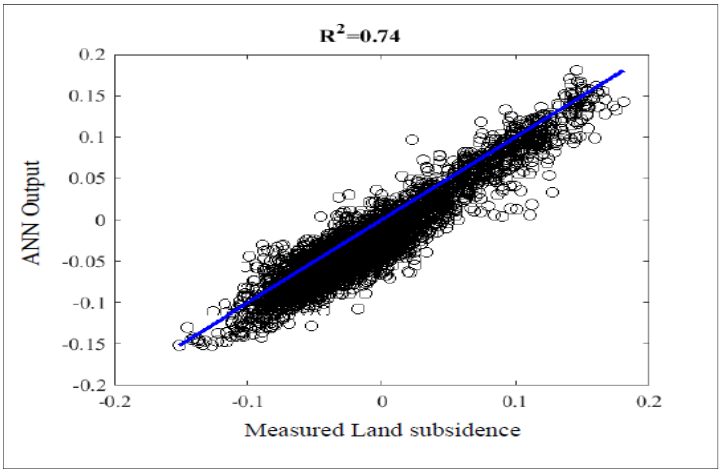

Figure 8. Relationship between the values obtained from the artificial neural network model and the measured subsidence values

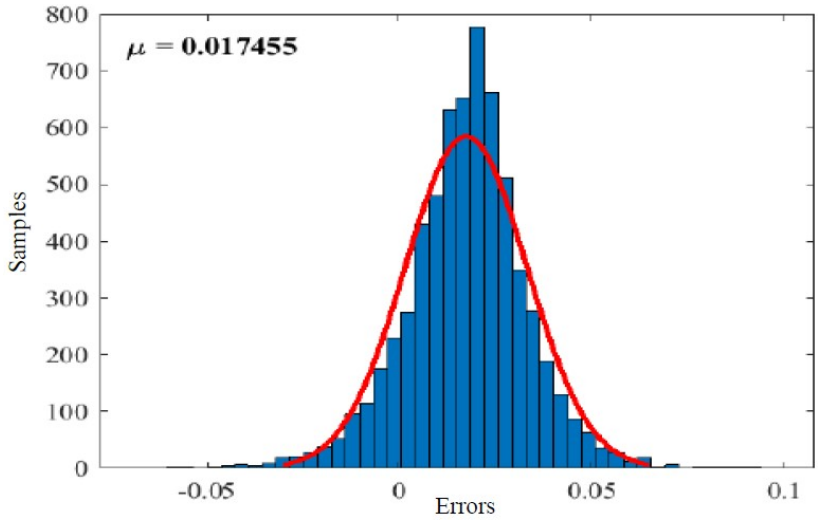

Figure 9. Histogram of error frequency

All graphs demonstrate the good performance of the ANN for modeling the Aliabad Land subsidence. It should be noted that in order to draw the graphs, the normalized outputs from the modeling have been returned to the original scale. At least, according to the mean square error, absolute mean error, coefficient of determination, and correlation coefficient which are almost equal for all data sets, the plunge trend of the performance graph of the neural network model can be considered as the reason for the good performance of the artificial neural network model.

Validation Techniques

In order to assess the validation of the ANN model, the land subsidence of some piezometers areas has been compared with the measured land subsidence by the InSAR technique from Sentinel-1 images from 2015 to 2016. Figure (11) compared the estimated land deformation by artificial neural network with the observed value of land elevation changes by satellite images in the study area of Aliabad plain of Qom. The maximum land subsidence in the study was computed at about 15 cm close to the central part of the plain with agricultural and residential land use. Also, the red points in figure (11-a) represent the points with phase ambiguity from differential radar interferometry that could not measure the land elevation.

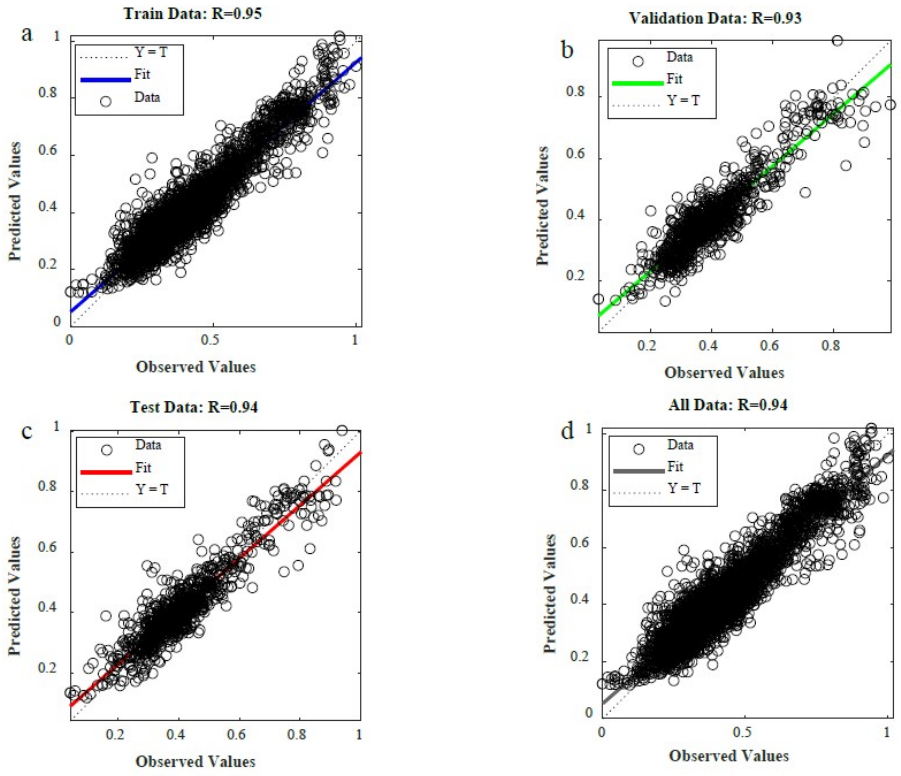

Figure 10. Results of ANN subsidence model. a) training b) validation c) test d) total data are given in comparison with real data

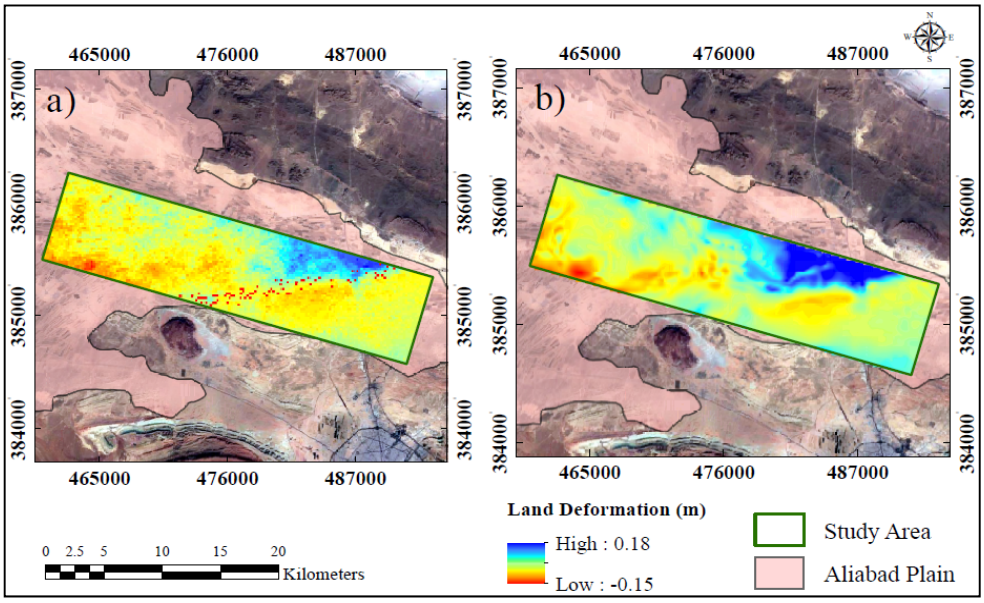

Figure 11. Comparison of a) the observed value of land elevation changes by satellite images with b) the estimated land deformation by artificial neural network

Following figure (12) illustrates a comparison between ANN model land elevation and the measured values from 2015 to 2016 in piezometers location. According to the obtained result in figure (12), the ANN model indicated a proper ability to understand the complex algorithms between independent parameters and modeled the land deformation with relatively good accuracy. In Addition, a comparison has been conducted between previous studies in the area

and the ANN results. To compare the results, the value of land subsidence in some piezometers has been investigated. Figure (13) indicates the rate of land subsidence in five piezometers P_5, P_7, P_{11}, P_{12}, and P_{13}. The results show that the ANN model is more sensitive to great changes in target value. In addition, the land subsidence rate in some piezometers has increased and in some others has decreased but it is persistently happening. Therefore, the land subsidence is continuous in the plain and the Aliabad aquifer is encountered groundwater mismanagement.

Test of the ANN model

The multi-layer neural network model that has been used in current study, have validated by using a new package dataset which did not used in training the model. The dataset includes all the same parameters of groundwater changes from 2009 to 2016 from distributed piezometers in the new study area, thickness of alluvial sediments, the coefficient of transmissivity, and elasticity modulus and land deformation from 2015 to 2016 of a new rectangular determined area that provided in figure (14). The relation between measured land elevation and predicted output of the ANN model could be seen in figure (15). The values of R=0.96 and R^2=0.91 demonstrate a high accuracy of prediction and the ability of extrapolation of the ANN model. In addition, according to table (2), the model estimated land deformation with the error value of 2 cm at each point that shows the model has the ability of generalization for unknown data of areas with the same geological, geotechnical, and hydrogeological features.

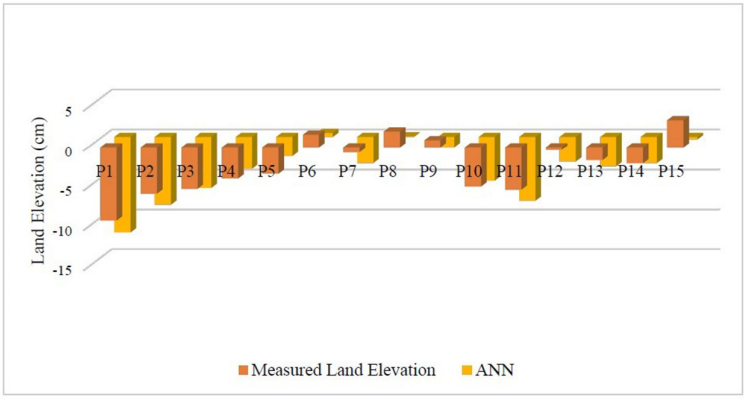

Figure 12. Comparison between ANN model land elevation and the measured in piezometers location

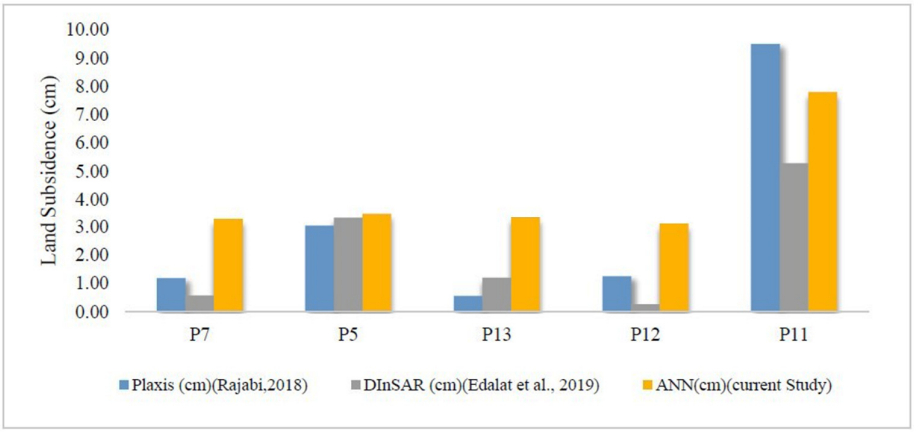

Figure 11. A comparison between ANN model of land subsidence and previous studies

Table 2. The results of validating ANN model

	R^2	R	RMSE(m)	MSE
Results	0.91	0.96	0.02	0.0004

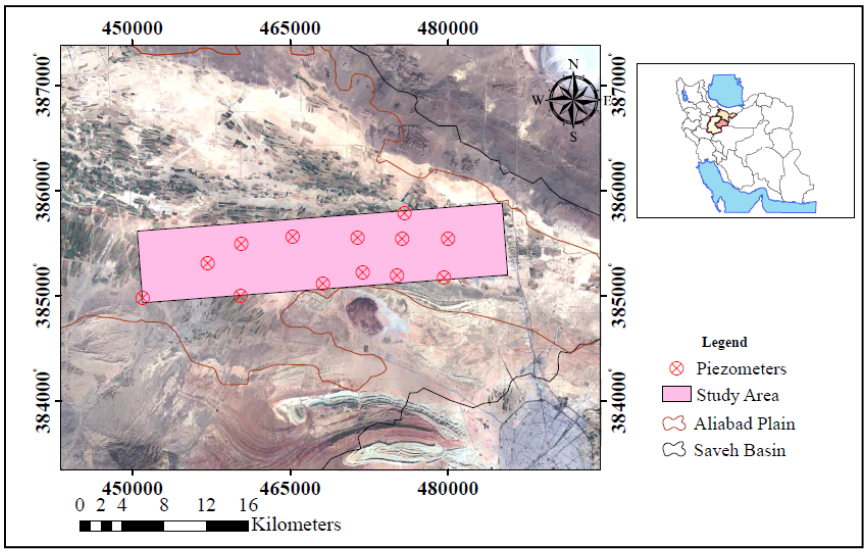

Figure 12. The area of validation data

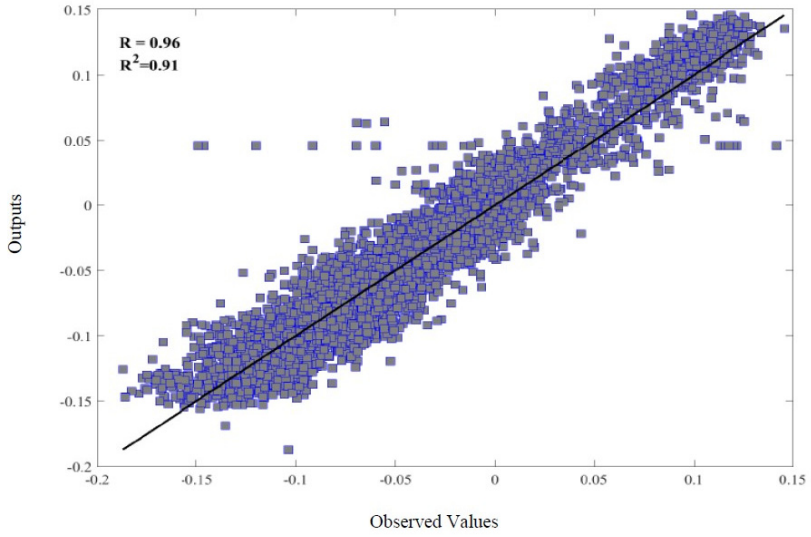

Figure 13. Relation between measured land elevation and predicted output of the ANN model

Sensitivity Analysis

In order to inquire into impaction of used input parameters, the sensitivity analysis has been applied. In this regard, the variable perturbation method has been used among the sensitivity analysis methods. For examining the effect of changes in each input value on the distribution of output, a perturbing by a quantity in parameters would be applied (Sueur et al., 2017). To perform the sensitivity analysis, one input parameter was multiplied by 0.5 and the other input parameters remained unchanged. This process is repeated for all four parameters. For evaluating the results, the value of R^2 was studied before and after the changes. Table (3), shows that groundwater changes have a significant impact on land deformation modeled. The given graph (Figure 16) helps to a better understanding of the input parameters effect.

Table 3. The results of sensitivity Analysis

Results	Elasticity Modulus	Groundwater Changes	Transmissivity Coefficient	Thickness of Sediments
before R^2		0.86		
After R^2	0.75	0.47	0.84	0.71
Difference R^2	-0.11	-0.39	-0.02	-0.15
The Absolute value of percentage changes of R^2	12.8	45.35	2.32	17.44

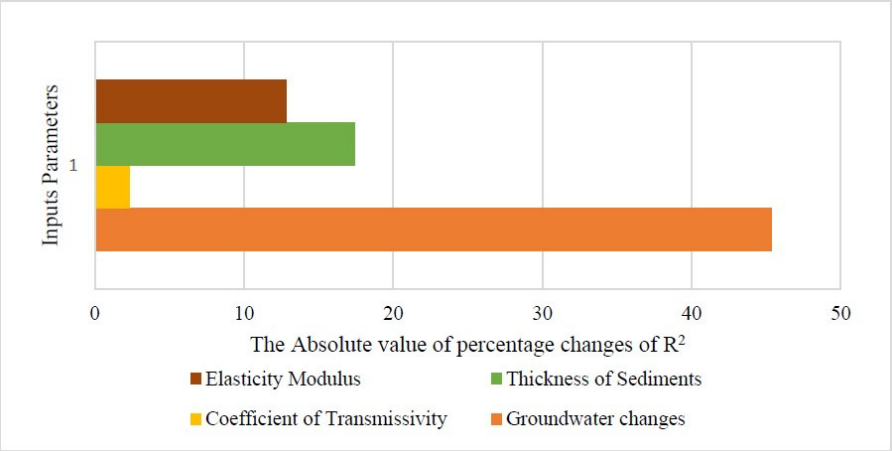

Figure 14. sensitivity Analysis

Conclusion

In this paper, the land subsidence of Aliabad plain of Qom from 2015 to 2016 is modeled by a three-layer perceptron artificial neural network. The ANN model for the prediction of land subsidence is developed using MATLAB R2018b software program. In order to train the model four variables including groundwater level dropdown, the thickness of alluvial sediments, the aquifer sediments' transmissivity, and elasticity modulus have been used as input parameters and measured land deformation as a single output parameter in the ANN model. The most considerable subsidence has occurred about 15 cm close to the central parts of Aliabad plain based on ANN results. In addition, sensitivity analysis results indicate the reduction of groundwater level has a significant impact on the land subsidence neural network model. Besides, the model has the ability to generalization and is able to predict land subsidence of a different part of the plain with new data set that are unused in the training process of the model.

References

Arabameri, A., Saha, S., Roy, J., Tiefenbacher, J. P., Cerda, A., Biggs, T., Pradhan, B., Ngo, P. T. T., Collins, A. L., 2020. A novel ensemble computational intelligence approach for the spatial prediction of land subsidence susceptibility. Science of The Total Environment.

Calderhead, A.I., Martel, R., Garfias, J., Rivera, A., Therrien, R., 2012. Sustainable management for minimizing land subsidence of an over-pumped volcanic aquifer system: tools for policy design. Water Resources Management, 1874-1864. https://doi.org/10.1007/s11269-012-9990-7

Calderhead, A.I., Therrien, R., Rivera, A., Martel R., Garfas, J., 2011. Simulating pumping induced regional land subsidence with the use of InSAR and field data in the Toluca valley Mexico. Advances in Water Resources, 34: 83-97.

Darvishzadeh, A., 1991. Geology of Iran. Amir Kabir, 873 pp. (In Persian).

Dave, V.S., Dutta, K., 2014. Neural network based models for software effort estimation: a review. Artificial Intelligence Review, 42: 295–307.

Dehghani, M., Nikoo, M.R., 2019. Monitoring and management of land subsidence induced by over-exploitation of groundwater. Advances in Natural and Technological Hazards Research, 48: 271-296.

Dehghani, M.,Valadan Zoej MJ, Entezam, I., 2013. Neural network modeling of Tehran land subsidence measured by persistent scatterer interferometry. Photogrammetrie-Fernerkundung-Geoinformation, 5-17.

Edalat, A., Khodaparast, M., Rajabi, A. M., 2019. Detecting land subsidence due to groundwater withdrawal in Aliabad plain, Iran, using ESA Sentinel-1 Satellite data. Natural Resources Research, 29: 1935-1950.

Edalat, A., Khodaparast, M., Rajabi, A. M., 2020. Scenarios to control land subsidence using numerical modeling of groundwater exploitation: Aliabad plain (in Iran) as a case study. Environmental Earth Sciences, 79 (494).

Galloway, D. L., Burbey, T., 2011. Review: Regional land subsidence accompanying groundwater extraction. Hydrogeology Journal, 1459-1486.

Galloway, D., Jones, D., Ingebritsen, S., 1999. Land Subsidence in the Unites States. US Geological Survey.

Gambolati, G., Teatini, P., 2015. Geomechanics of subsurface water withrawal and injection. Water Resources Research, 3922-3955.

Gunn, S.R., 1998. Support vector machines for classification and regression, Technical Report, University of Southampton, UK.

Hu, B., Wang, J., Chen, Z., Wang, D., Xu, S., 2009. Risk assessment of land subsidence at Tianjin coastal area in China. Environmental. Earth Sciences, 59: 269-276.

Hu, R.L., Yue, Z.Q., Wang, L.C., Wamg, S.J., 2004. Review on current status and challenging issues of land subsidence in China. engineering geology, 76: 65-77.

Jahangir, M. H., Khosravi, Z., Sarrafha, H., 2020. Modeling of land subsidence due to groundwater overexploitation using elastoplastic mohr-coulomb model in Arak plain, Iran. Geopersia.

Jayalakshmi, T., Santhakumaran, A., 2011. Statistical normalization and back propagation for classification. International Journal of Computer Theory and Engineering.

Kia, S. M., 2016. Neural network in Matlab. Kian. Tehran. (In Persian)

Knudby, A., Brenning, A., LeDrew, E., 2010. New approaches to modelling fish-habitat relationships. Ecological Modeling, 221 (3): 503-511.

Lixin, Y., Fang, Z., He, X., Shijie, C., Wei, W., Qiang, Y., 2011. Land subsidence in Tianjin, China. Environmental Earth Sciences, 62: 1151-1161.

Mahmoudpour, M., Khamehchiyan, M., Nikudel, M.R., Ghassemi, M.R., 2015. Numerical simulation and prediction of regional land subsidence caused by groundwater exploitation in the southwest of Tehran, Iran. Engineering Geology. Doi: 10.1016/j.enggeo.2015.12.004

Motagh, M., Djamour, Y., Walter, T., Wetzel, H.-U., Zschau, J., Arabi, S., 2007. Land subsidence in Mashhad valley, northeast Iran: results. Geophysical Journal International, 518-526.

Mousavi., M., Shamsai, A., El Naggar, M. H., Khamechian, M., 2001. A GPS-based monitoring program of land subsidence due to groundwater withdrawal in Iran. Canadian Journal of Civil Engineering,452-464.

Na, T., Kawamura, Y., Kang, S.S., Utsuki, S., 2021. Hazard mapping of ground subsidence in east area of Sapporo using frequency ratio model and GIS. Geomatics, Natural Hazard and Risk, 347-362.

Oh, Hj., Ahn, SC., Choi, JK., Lee, S., 2011. Sensitivity analysis for the GIS-based mapping of the ground subsidence hazard near abandoned underground coal mines. Environmental Earth Sciences, 64: 347-358.

Phien Wej, N., Giao, P. H., Nutalaya, P., 2006. Land subsidence in Bangkok, Thailand. Engineering Geology, 82:187-201.

Pirouzi, A., Eslami, A., Kharaghani, S., TavousiTafreshi, S., 2014. Analytical and experimental study of land subsidence in south western area of Tehran. Vitae Columbia, 21 (1): 233-254.

Rahmani, Y., Ahmadi, F., 2018. Application of InSAR in measuring earth's surface deformation causedby groundwater extraction and modeling its behavior using timeseries analysis by artificial neural networks, 1171-1184.

Rajabi, A. M., 2018. A numerical study on land subsidence due to extensive overexploitation of groud water in Aliabad plain, Qom-Iran. Natural Hazard.

Rajabi, A. M., Ghorbani, E., 2016. Land subsidence due to groundwater withdrawal in Arak plain, Markazi province, Iran. Arabian Journal Geosciences.

Sueur, R., looss, B., Delage, T., 2017. Sensitivity analysis using perturbed-Law based indices for quintiles and application to an industrial case. arXiv.

Taravatrooy, N., Nikoo, M. R., Sadegh, M. P., 2018. A hybrid clustering-fusion methodology for land subsidence estimation. Natural Hazard, 905-926.

Todd, D. K., Mays, L. W., 2005. Groundwater Hydrology. Third Ed., John Wiley and Sins Inc., U.S.A. 636p.

Water Resources Report of Saveh Study Area., 2013. Iran water resources management. Water Utility Company in Qom: Abkhan Consulting Engineers (in Persian).

Zamani-Pedram, M., Hosseini, H., Jafarian, B., 2002. Geological Map of Qom. Geological Survey of Iran scale 1:1,000,000. (in Persian)

Zhao, Y., Wang, C., Yang, J., Bi, J., 2021. Coupling model of groundwater and land subsidence and simulation of emergency water supply in Ningbo urban area, China. Journal of Hydrology.